MODEL FIRES OF REFUSE DERIVED FUELS: TEMPERATURE PROFILES AND PYROLYSATE FLUX

Samorn Hirunpraditkoon, Bogdan Z. Dlugogorski and Eric M. Kennedy

Process Safety and Environment Protection Research Group
School of Engineering
The University of Newcastle
Callaghan, NSW 2308, Australia
Email: Bogdan.Dlugogorski@newcastle.edu.au
Fax: +61 2 4921 6920

ABSTRACT

This study presents the experimental measurements of temperature profiles and temperature histories within specimens of surrogate refuse derived fuels (RDFs) exposed to irradiance in a cone calorimeter. The surrogate RDFs, representing typical municipal solid waste collected in the city of Newcastle, Australia, were developed to improve the reproducibility of experimental measurements. These materials consist of loose polydispersed particles of grass, wood, paper, plastic, bread and sugar. A specialised sample holder was constructed to accommodate four fine thermocouples (76 μm in diameter), which facilitated measurement of the temperature profiles within RDF samples undergoing oxidation and pyrolysis. An additional thermocouple was positioned at the base of the sample to verify the assumption of heat transfer in a semi-infinite slab, prior to ignition. This assumption was applied previously within the context of integral analysis to obtain a value of the effective thermal conductivity. The temperature profiles prior to ignition were combined with measurements of the surface temperature collected by the pyrometer. Mass-loss measurements were performed, but only after the onset of the flaming combustion, as a consequence of flow-field induced fluctuations. A separate data-acquisition system was used to allow a faster sampling rate than 1 Hz permitted by the default setting of the cone calorimeter. The experiments determined the critical mass flux at extinction and identified three combustion regimes occurring in fires of RDF-type materials: i) flaming combustion, ii) a transitional regime involving simultaneous flaming combustion and char pyrolysis, and iii) char pyrolysis. The measurements were consistent with results of the earlier fire experiments performed in the cone calorimeter.

INTRODUCTION

The purpose of this paper is to report the measurements of the development of temperature profiles within the RDF samples and mass changes of RDF samples as a result of pyrolysis and char oxidation. All measurements were performed in the cone calorimeter, with major modifications performed to the instrument, including modification of the sample holder and the data acquisition system.

Temperature measurements are divided into pre- and post-ignition periods. This is done for convenience in reporting the experimental data and to highlight differences in the pre- and post-ignition heat transfer regimes in the RDF samples. During the pre-ignition period, a steep temperature profile develops in the material near its top boundary, although within the

sample itself, the temperature remains unchanged. The pre-ignition measurements allow one to confirm the thermally-thick approximation, providing a complete picture of the heat transfer in RDF samples prior to ignition.

After ignition, following the attrition of the RDF material, the top thermocouples become progressively exposed in the gas phase and may no longer track the material's true temperature. Also, following the cessation of flaming combustion, the thermocouples remaining in the material show a substantial, though relatively slow, increase in temperature. This effect occurs as a consequence of the shift in the kinetic regime in the samples, from endothermic pyrolysis reactions to exothermic char oxidation.

The temperature results are complemented by the measurement of the mass-loss rate, which reflect the volume-average rate of pyrolysis and char oxidation in the RDF samples. These measurements were performed for three sample densities, but only for the samples of 40 mm in thickness, to circumvent laboratory difficulties encountered in experiments with thinner samples. The mass-loss measurements were converted to mass-flux data by differentiating the mass-loss curves and then dividing the results by the area of the opening of the sample holder. This permits one to obtain estimates of critical mass fluxes at ignition and extinction of the RDF material.

MEASUREMENT OF TEMPERATURE PROFILES

Experimental Apparatus

The experiments to measure the evolution of the temperature profiles in the samples were conducted in a mass-loss calorimeter. The instrument consisted of a heating element, with its temperature regulated by the Eurotherm 847 controller, and a strain gauge for obtaining the mass-loss measurements. Although, the mass-loss data were not recorded in the present series of experiments, the entire rig was nonetheless denoted for convenience as the mass-loss cone calorimeter. The specimens and their preparation were described in detail by Hirunpraditkoon et al. (2004) and Dlugogorski et al. (2004). This description will not be repeated here.

The sample holder was of standard size, 100 x 100 mm in area, 50 mm in height, with an exposed surface area of 0.0088 m^2, and operated only in the horizontal orientation. The sample holder was instrumented with five chromel-alumel (Type K) thermocouples, all made of wires of 76 μm in diameter. Holes were drilled through the holder's walls to allow the top four thermocouples to be positioned 3, 8, 13 and 23 mm below the surface of the samples, as illustrated schematically in Figure 1. The fifth thermocouple was placed at the bottom of the sample holder to measure the temperature at the base of the sample.

Tubes made of alumina (o.d. 1.6 mm, i.d. 0.79 mm) were passed through the holes, providing insulation between the thermocouple wires and the sample holder. Note that a double-hole alumina insulator (o.d. 1.6 mm, i.d. 0.40 mm) was used for the bottom thermocouple. Within the central portion of the thermocouple wires, about 2.5 cm on each side of the thermocouple junction, the thermocouple wires were not insulated by the alumina tubes. This was done to minimise the thermal inertia of the thermocouple set-up and to avoid conduction losses between the thermocouple junction and the alumina insulator.

For the experiments conducted prior to ignition, the analogue signal of the five thermocouples was digitised at the frequency of 200 Hz (5 ms intervals) by the same data collection system used to record the surface temperature measured by the pyrometer (Dlugogorski et al., 2004). This system consisted of a PC computer equipped with a PCI-6024E data acquisition card and running the Labview software. Both the pyrometer and the thermocouple measurements were gathered simultaneously allowing one to compile the temperature profile in the sample prior to ignition.

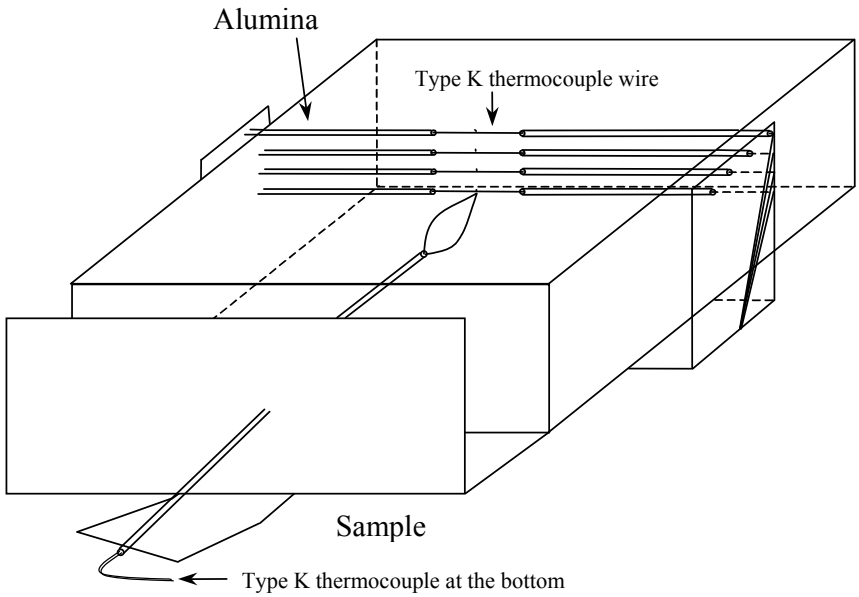

Figure 1: Schematic diagram of the modified sample holder with the thermocouple assembly.

Following ignition, flames could damage the pyrometer and the measurement of the surface temperature could not be continued (Dlugogorski et al., 2004). Thus after ignition, only the temperature histories recorded with thermocouples are reported in this paper. In this regime, the experimental runs were much longer, in the order of 500 s, as compared to 20 s before the ignition. Although the same data acquisition system was deployed in the post-ignition series of experiments, the frequency of sampling was reduced to 10 Hz. The measurement of the temperature profiles continued for about 150–200 s after completion of flaming combustion. For example, at the irradiance level of 20 kW m^{-2}, the flame extinguished at between 200 and 250 s, and the data collection was continued until 400 s. At the irradiance level of 45 kW m^{-2}, the flame extinguished between 400 and 450 s necessitating longer experimental runs, up to 600 s in duration.

Temperature Profiles Prior to Ignition

Figures 2 and 3 illustrate replicated temperature profiles within the RDF material at ignition (L = 40 mm, ρ = 50 kg m^{-3}) for the irradiance levels of 20 and 45 kW m^{-2}. At each irradiance level, at least four replicates were obtained. The time to ignition (t_{ig}) and the surface temperature at ignition (T_{ig}) for each replicate are tabulated in the inserts in Figures 3 and 4, together with the typical error bars in the thermocouple measurements. The temperatures at

the top of each sample (L = 0) are those measured with the pyrometer, as described by Dlugogorski et al. (2004). One can readily notice from these figures that the thermally-thick assumption applies well prior to ignition, even for the samples of 12.5 mm in thickness. This means that a thermal wave propagating into the material does not encounter the bottom boundary and the material, for the purpose of the heat-transfer calculations, can be considered as a semi-infinite slab, at all times before ignition.

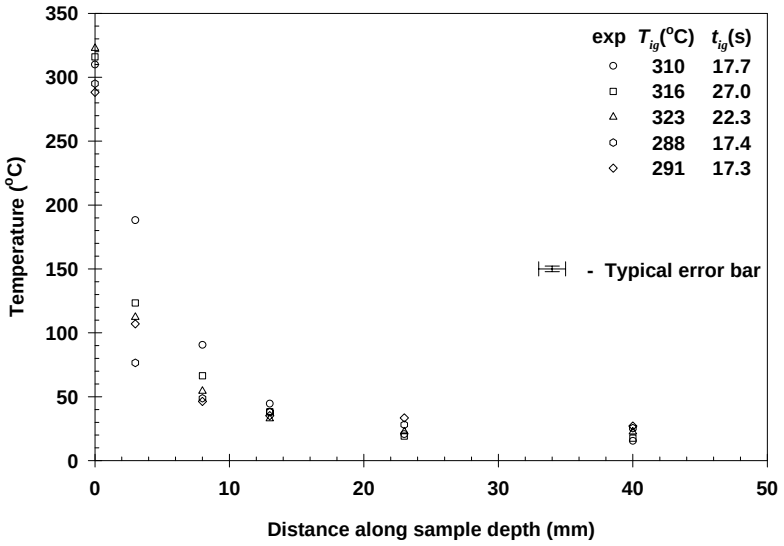

Figure 2: Replicates of the temperature profile at ignition for oven dried surrogate RDF, L = 40 mm, ρ = 50 kg m^{-3} and $\dot{q}''$ = 20 kW m^{-2}.

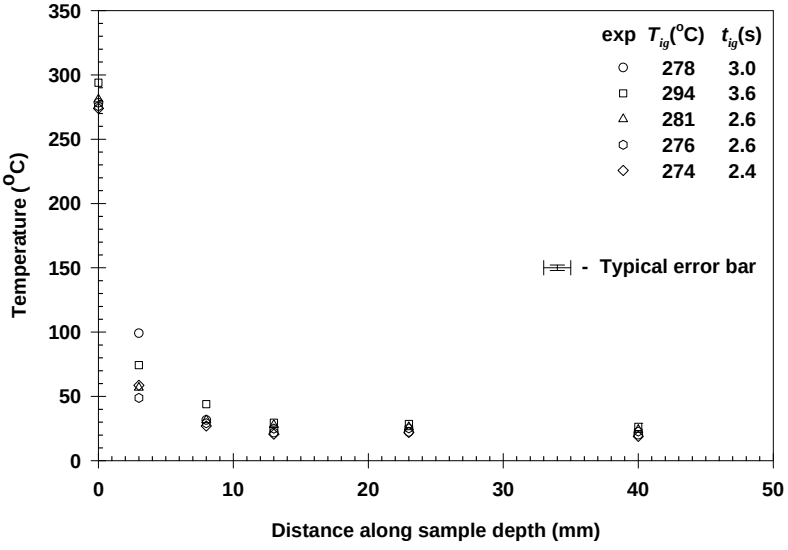

Figure 3: Replicates of the temperature profile at ignition for oven dried surrogate RDF, L = 40 mm, ρ = 50 kg m^{-3} and $\dot{q}''$ = 45 kW m^{-2}.

Figure 2 shows that significant scatter in the experimental results occurs at measuring positions 3 and 8 mm inside the material. The scatter in the data obtained at $\dot{q}'' = 45$ kW m^{-2} is not as apparent. Note that at 20 kW m^{-2} it takes 6–8 times as long for a sample to ignite as it takes for samples exposed to irradiance of 45 kW m^{-2}. It is possible that the heterogeneous nature of the material leads to a temperature field, which depends locally on the material composition. The heterogeneities may include different types of materials, different particle sizes and different void fractions. Similar temperature profiles, before ignition, were obtained for planed wood, paper and grass (Hirunpraditkoon, 2003).

Temperature Histories

The results obtained for the temperature histories within the RDF samples are shown in Figures 4 and 5 for irradiance levels of 20 and 45 kW m^{-2}, respectively. The temperature measurements in the experiments were affected by electromagnetic interference (spikes) induced by the cone, as shown in the top section of Figures 4 and 5. The spikes were manually removed to generate the smooth temperature histories, corrected for electromagnetic interference, as illustrated in the bottom part of Figures 4 and 5. The current experimental measurements are presented in terms of the temperature evolution with time, at each measuring station. Because of this consideration, these measurements are denoted as the temperature histories rather than the temperature profiles. The shapes of the temperature histories at various stations are similar to those published by other researchers for wood, e.g. Kashiwagi et al. (1987).

The specimens burned more intensely at the edges than at the centre of the sample, leading to the sample surface receding faster at the edges. It is believed that this phenomenon caused tensioning of the thermocouple wires and eventually contributed to the breakage of thermocouples 1 and 2, as illustrated in Figure 5. The temperature histories before ignition are plotted in Figure 6 for the irradiance of 45 kW m^{-2}; the results for the irradiance of 20 kW m^{-2} are presented by Hirunpraditkoon (2003). The measurements in Figure 6 were obtained in separate experiments from the measurements illustrated in Figure 4. Note that the surface temperature histories illustrated in Figure 6 are derived from the pyrometer readings (Dlugogorski et al., 2004).

It is evident that very little heating takes place within the specimens prior to ignition, and the heat wave propagates substantially into the material only after the ignition. Before ignition, the temperature rise close to the surface of the sample may be in part due to the exothermic reactions between oxygen and the carbonaceous components of RDF, as reported for wood by Kashiwagi et al. (1987).

The temperature profiles within the samples (compare Figures 4 and 5 at the same instant) depend on the incident heat flux. High irradiances result in more elevated temperatures, as a consequence of increased heat input into the samples and more rapid oxidation of char. The effect of char oxidation can be seen at longer times by comparing the temperature histories at the lowest measuring station in Figures 4 and 5. But char oxidation can also increase the temperature at other locations closer to the surface of the sample (Urbas and Parker, 1993), and result in emission of carbon monoxide. The latter observation is consistent with the carbon monoxide measurements reported by Hirunpraditkoon et al. (2004).

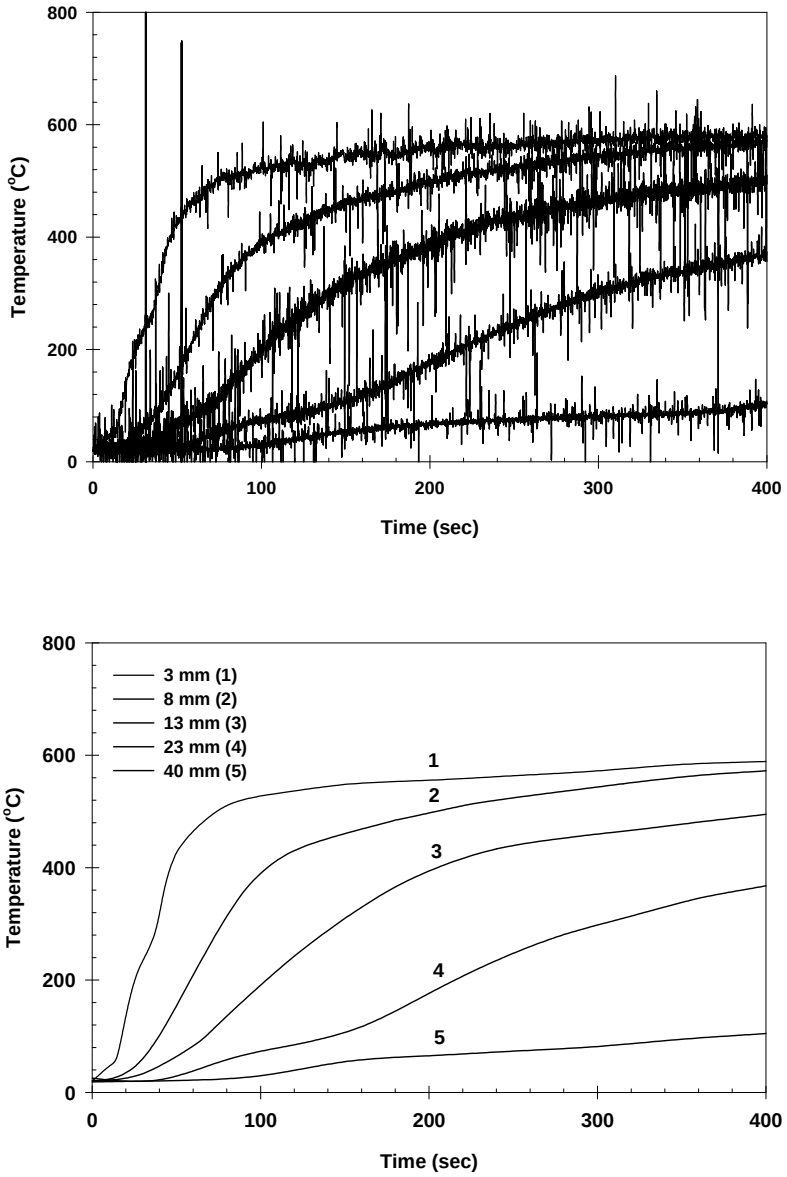

Figure 4: Transient temperature distributions of 40 mm in thickness and 50 kg m^{-3} in density of oven dried surrogate RDF samples, at an irradiance level of 20 kW m^{-2}: (a) raw experimental data, with electromagnetic interference; (b) smoothed curves.

A noticeable temperature plateau around 100 °C can be seen for both the low and high heat fluxes of surrogate RDF. This plateau is found at locations of 23 and 40 mm from the sample surface at both irradiance levels of 20 and 45 kW m^{-2}. Although the samples were initially dry, they are very hygroscopic and might have accumulated moisture when they were charged into the sample holder. The plateaus were not observed at positions 1–3 (Figures 4 and 5), which is consistent with the observation of Kashiwagi et al. (1987) who argued that close the sample surface the heating rate is too fast for this plateau to become noticeable. It is also reasonable to suggest that the moisture present at the bottom of the sample migrated there

from the pyrolysing RDF close to the surface, early in the combustion process. Such a phenomenon was reported by Dlugogorski et al. (2002) for the combustion of cardboard under fire conditions.

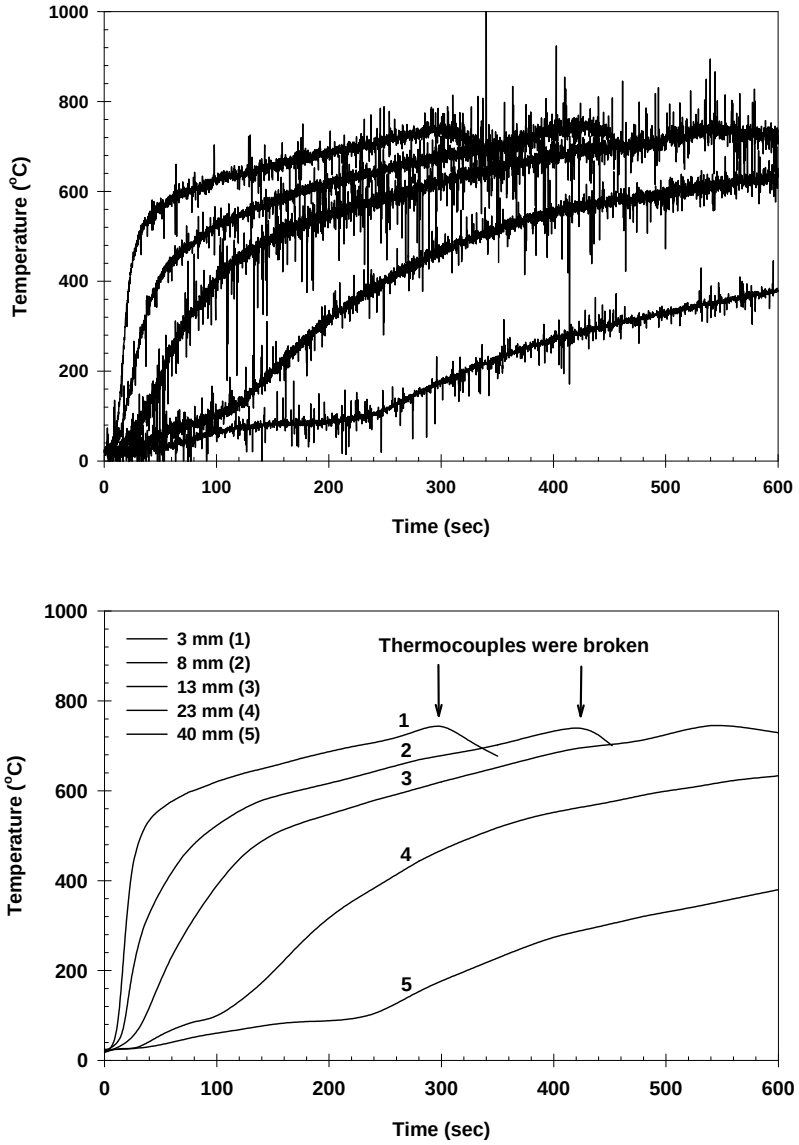

Figure 5: Transient temperature distributions of 40 mm in thickness and 50 kg m^{-3} in density of oven dried surrogate RDF samples, at an irradiance level of 45 kW m^{-2}: (a) raw experimental data, with electromagnetic interference; (b) smoothed curves.

MASS LOSS AND MASS FLUX RESULTS

Experimental Apparatus

The mass-loss results were obtained from model fires experiments conducted in the cone calorimeter. The mass flux rates, that is, the mass per unit surface and per unit time,

correspond to the slope of the mass loss curve divided by the surface area of the sample holder (0.0088 m^2). These data allow one to investigate the pyrolysis rates during flaming combustion and permit the estimation of the rates of char oxidation during smouldering. It will be argued in the next section that, combustion of thicker and more dense RDF samples under fire conditions leads to the emergence of a transitional period, characterised by simultaneous flaming combustion and char oxidation. In this period, the results presented here provide an estimate of the overall mass loss of an RDF sample.

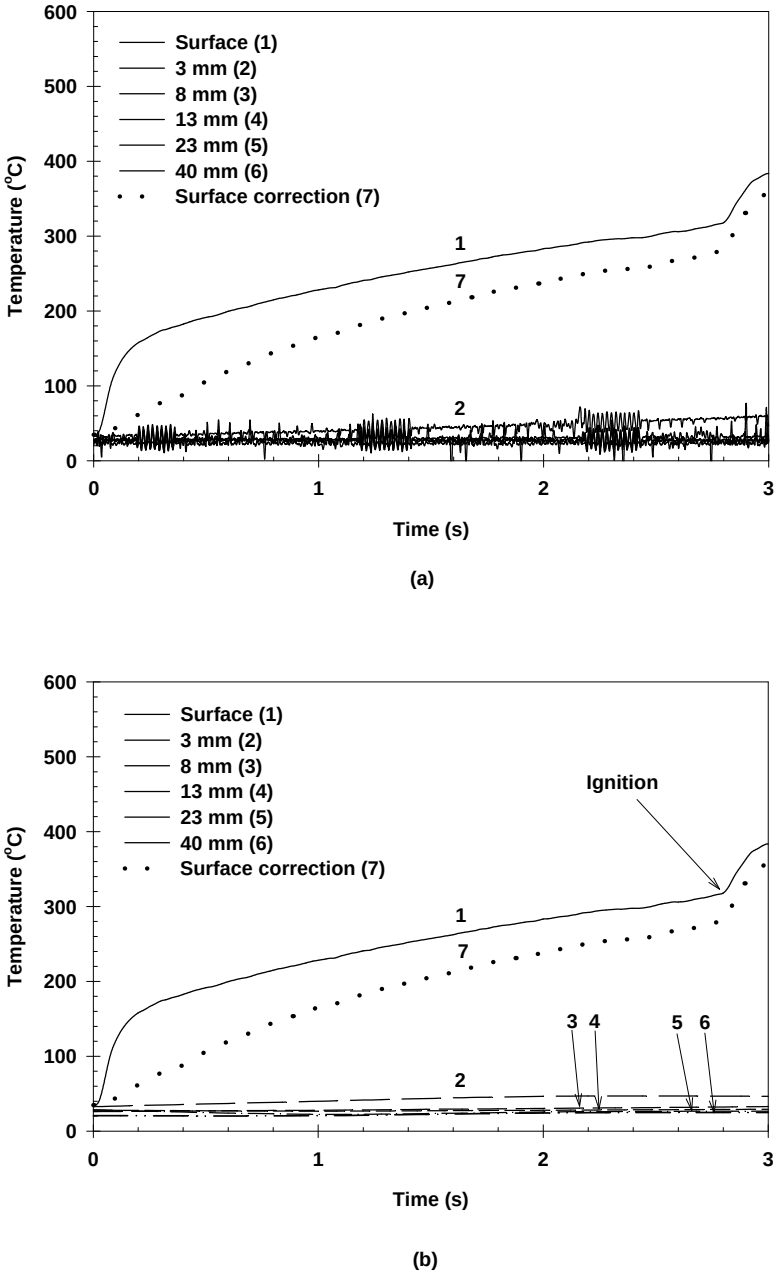

Figure 6: Temperature histories recorded by the pyrometer and temperature inserted within oven dried surrogate RDF samples, at L = 40 mm, ρ = 50 kg m^{-3} and $\dot{q}''$ = 45 kW m^{-2}: (a) raw data with electromagnetic interference; (b) smoothed curves.

Experiments were performed at three irradiance levels (30, 40 and 50 kW m^{-2}), for three nominal sample densities (37.5, 50 and 62.5 kg m^{-3}), and for one sample thickness (40 mm). The standard data acquisition system of the cone calorimeter is capable of digitising the analogue signal of the strain gauge at a maximum frequency of 1 Hz. To avoid this limitation, the signal from the strain gauge was logged by a PCI-6024E/Labview 5.0 system at 10 Hz. The measurements were collected over 800 s during each experiment.

Experimental Measurements

The experimental results are summarised in Figure 7 in terms of mass loss and in Figure 8 in terms of mass flux. The data are presented only after the onset of flaming combustion. Because of the rapid mass fluctuations induced by the expanding flame at the point of ignition, it was not possible to obtain reliable results prior to ignition. In the figures, the results for each irradiance level (30, 40 or 50 kW m^{-2}) are grouped together. It can be readily seen that, following ignition, the sample mass decreases rapidly due to pyrolysis, especially for samples of the lowest density (37.5 g m^{-3}); see Figure 7. The rate of mass change (mass flux) declines as well (Figure 8), owing to the increasing limitations in mass and heat transfer within the specimens due to the accumulation of char and longer path for diffusion of pyrolysates. Note that the mass flux declines monotonically following ignition. This is consistent with the oxygen-consumption measurements presented by Hirunpraditkoon et al. (2004) that show no second peaks in the curves of heat release rate. After the cessation of flaming combustion, the sample mass continues to decline, but at a much slower rate, indicating char oxidation.

For each experiment, the mass of the sample at ignition and extinction is indicated in the legend to Figure 7. The mass flux, at these two points, is shown in the legend to Figure 8. With respect to the results shown in the legend to Figure 7, the percentage of the material removed prior to extinction is approximately constant (68%), and no trends can be discerned as to the influence of sample density or the irradiance level, above the background level of the experimental scatter. This means that the mass released by RDF specimens prior to extinction is limited by the total amount of fuel available in the samples. On the other hand, the mass flux after at the point of ignition shows an upward trend with increasing the incident radiative heat flux (Figure 8 at $t = 0$). This is why the peak heat release rate, which occurs shortly after ignition of the RDF samples, tends to increase with the incident radiative flux, as illustrated in Hirunpraditkoon et al. 2004). The mass flux at the point of extinguishment of the flaming combustion decreases with increasing sample density and increasing heat flux.

In several experiments, especially with higher-density and thicker samples, it was observed that the periods of flaming and smouldering combustion were not well separated by a point of flame disappearance. Rather, toward the end of the flaming combustion, the flames remained anchored only over a part of the specimen's surface allowing oxygen to diffuse to the surface of the remaining part of the sample. This did not happen in thinner and less dense samples, resulting in more rapid extinguishment, once an insufficient quantity of the decomposition products was delivered to the gas phase to sustain flaming combustion.

After ignition, the mass loss of RDF proceeds through three regimes: pyrolysis, pyrolysis and char oxidation (transitional regime) and char oxidation. If extinguishment arises in the regime where the contribution of char oxidation to the total heat release rate is small, the mass flux at extinction is constant, around 1.5–1.9 g m^{-2} s^{-1}, with the variation due to the experimental

scatter. However, if extinguishment takes place in the regime characterised both by pyrolysis and char oxidation, the critical mass flux at extinction varies over a wider range, between 0.8 and 1.5 g m^{-2} s^{-1}. We suggest that the overlap between pyrolysis and char oxidation is the result of the multicomponent and polydisperse nature of the surrogate RDF, which allows the two combustion regimes to exist concurrently within a heterogenous sample.

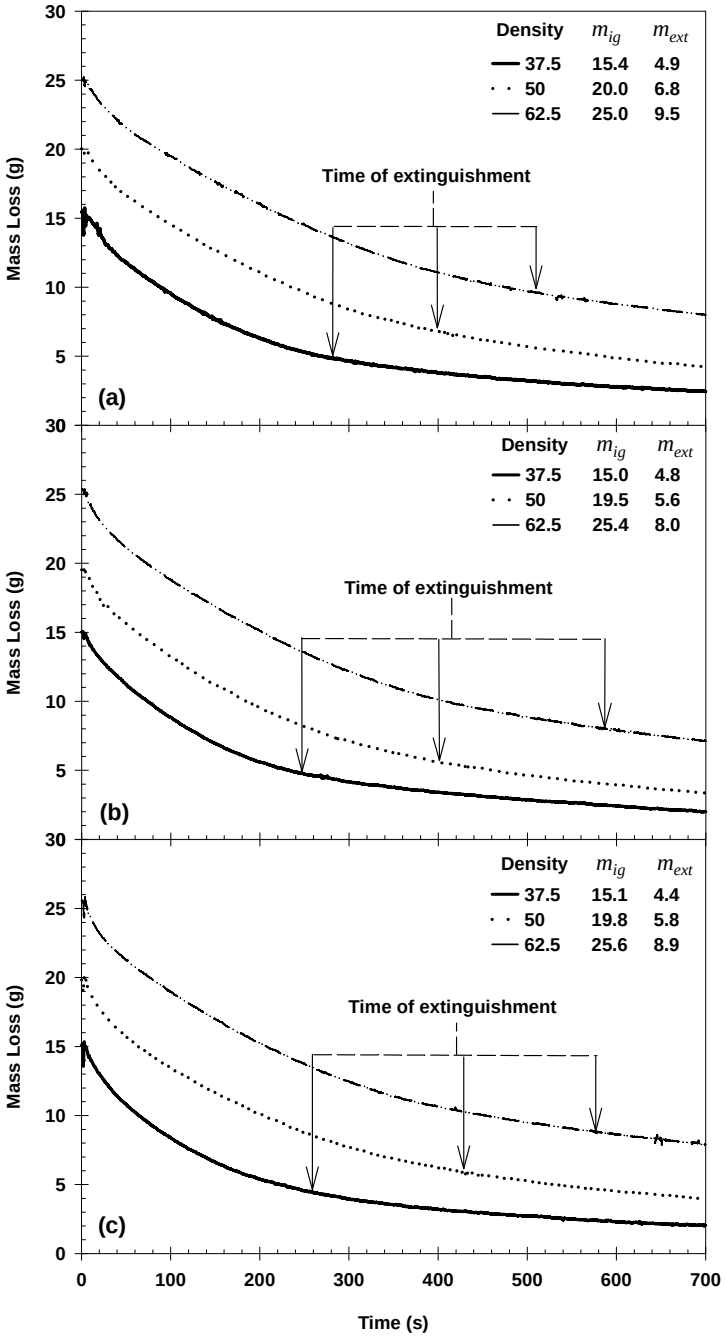

Figure 7: Mass loss histories of oven surrogate dried RDF, starting from the time of ignition, for three different densities at 40 mm in thickness and the three different irradiance levels: (a) 30 kW m^{-2}; (b) 40 kW m^{-2}; (c) 50 kW m^{-2}.

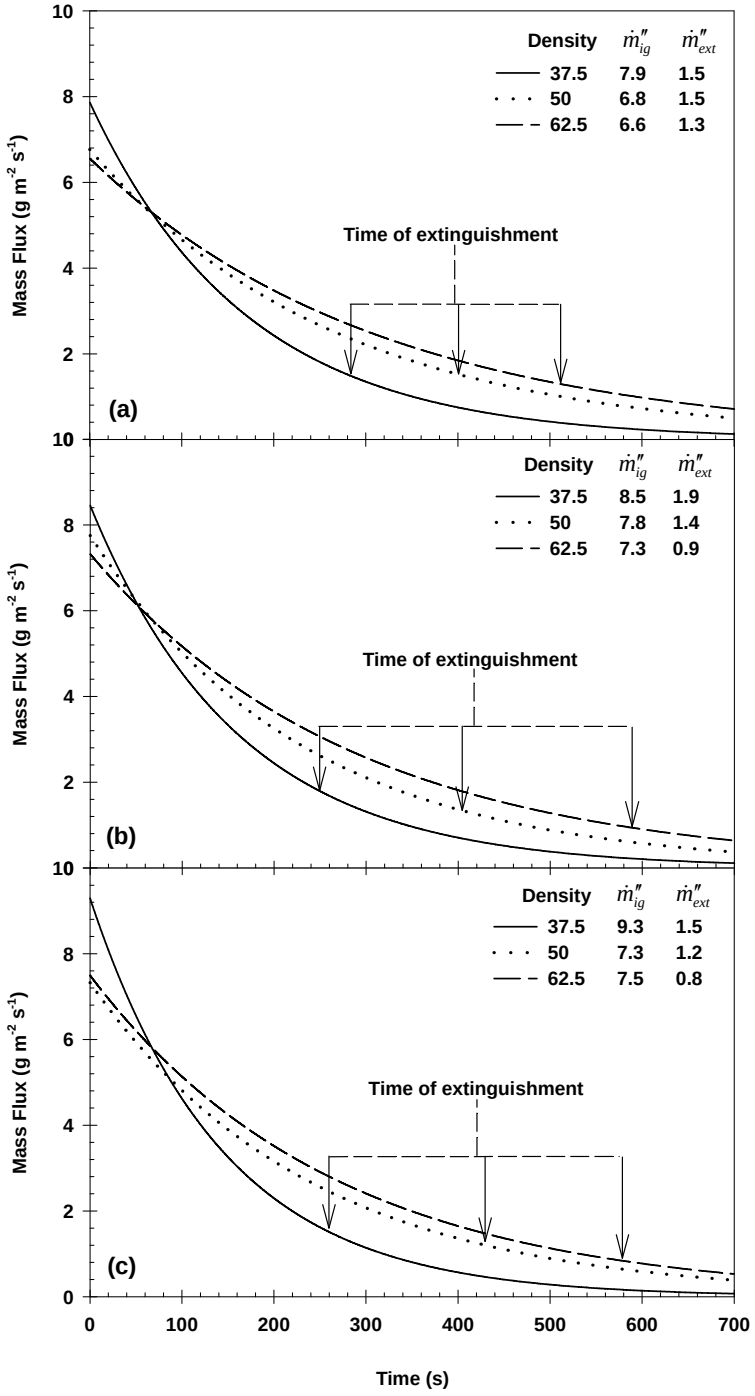

Figure 8: Mass flux histories of oven dried surrogate RDF, starting from the time of ignition, for three different densities at 40 mm in thickness and the three different irradiance levels: (a) 30 kW m^{-2}; (b) 40 kW m^{-2}; (c) 50 kW m^{-2}.

CONCLUSIONS

This paper presented experimental measurements of (i) the temperature profiles and temperature histories before and after ignition, as well as (ii) mass loss and mass flux results of RDF samples exposed to the irradiant fluxes in the cone calorimeter. The temperature profiles prior to ignition display a steep temperature rise near the material's surface and very little temperature variation inside the specimens. This proves the validity of the conjecture that RDF can be considered thermally thick as it was assumed, within the context of the integral analysis, presented by Hirunpraditkoon et al. (2004).

Heterogeneities in RDF, such as different type of materials, different particle sizes and different (local) void fractions, lead to variation in the temperature profiles observed in replicated experiments. The temperature histories in the samples are similar in shape to those published in the literature, which were interpreted by other researchers to indicate the presence of exothermic reactions occurring prior to ignition. The imposed radiative heat flux influences the temperature histories inside RDF samples, and affects the rate of the pyrolysis and especially the rate of the char-oxidation reactions.

As a consequence of fluctuations in the readings of the strain gauge, no mass loss results (pre-ignition oxidation and pyrolysis) were derived from the measurements prior to ignition. After ignition, both mass-loss and mass-flux curves decrease monotonically. This observation is consistent with the results reported by Hirunpraditkoon et al. (2004), which indicated no second peak in the HRR curves of the surrogate RDF. The amount of material removed by pyrolysis and oxidation prior to extinguishment is approximately 68% and appears independent of sample thickness, its density and the imposed irradiance. This may be the result of the high void fractions exhibited by the RDF materials studied, which inhibit the formation of a continuous layer of char during combustion.

The critical mass flux at extinction varies between 0.8 and 1.5 g m^{-2} s^{-1} for samples that extinguish in the transitional regime, and 1.5–1.9 g m^{-2} s^{-1} for thinner and less dense samples for which the transitional regime is not well articulated.

REFERENCES

Dlugogorski B. Z, Wang H., Kennedy E. M. and M. A. Delichatsios (2002) "Testing of gaseous fire suppressants in narrow channel apparatus." *Proc Halon Options Technical Working Conference*, Albuquerque NM, USA, NIST Special Publication: **984**: 1-11.

Dlugogorski B. Z. Hirunpraditkoon S. and E. M. Kennedy (2004) "Ignition of heterogenous loosely packed materials", submitted.

Hirunpraditkoon (2004) *Fire Properties of Refused-Derived Fuels*, PhD Dissertation, The University of Newcastle, Australia.

Hirunpraditkoon S., Dlugogorski B. Z. and E. M. Kennedy (2004) "Fire properties of surrogate refuse-derived fuels", submitted.

Kashiwagi T., Ohlemiller T. J., and K. Werner (1987) *Combustion and Flame* **69**, 331-345.

Urbas J. (1993) *Fire and Materials* **17**, 119-123.